On-going Validation of NeoNarval

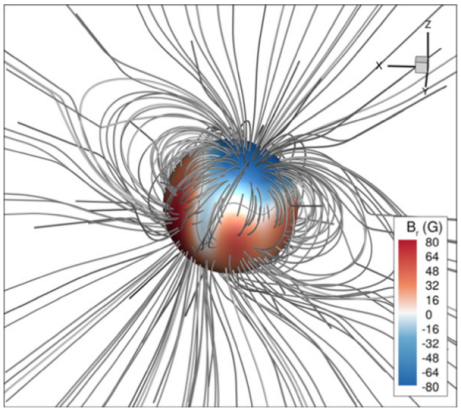

A. López Ariste, Ph. Mathias

December 15, 2024

Contents

Key points in this document

- The optical resolution of the instrument is 52000. The goal of NeoNarval was a resolution of 65000. **The DRS mathematically recovers this final resolution of 65000**.
- Absolute wavelength calibration is made with 50 m/s variance per line, and **2m/s global precision**.
- β CrB is a well-known magnetic calibration star. Its inclined dipole results in a well-determined sinusoidal variation of the measured Stokes V signal with amplitude corresponding to 500G. **The superposition of 10 years of data folded in rotational phase of Narval and NeoNarval is just indistinguishable.**
- Simultaneous observations of linear polarization of Betelgeuse with Espadons-CFHT and NeoNarval show **indistinguishable profiles at better than** 10^{-4}**.**
- The **Stokes V signal** of Vega shows the same amplitude (10^{-5}) and polarity in 2023 (Neo-Narval) than in 2009 (Narval), **at better than** 5×10^{-6}.
- After a change in the cooling system, **velocimetry is made now with 3 m/s noise.**
- The following cases cite calibration data but also **published results for Stokes V** (EK Dra), linear polarization (Betelgeuse) and intensity profiles Altair.

Part I

Instrumental calibration

Spectral resolution

The spectral resolution of NeoNarval must be 65000 all over the orders, matching the spectral resolution of Narval.

The DRS implements innovative machine learning algorithms that bring up the optical resolution of 52000 to the requested 65000.

The change of the detector in NeoNarval brought up larger pixels in an otherwise almost unchanged spectral image. The instrument resolution was degraded by this change to 52000. This subsequent loss in optical resolution had to be corrected during the spectral extraction by the DRS, using super-resolution techniques. An oversampled spectra is proposed as solution to the deconvolution problem. Sparse regularization keeps the high frequencies from being dominated by noise. Along-the-slit redundancy allows these high frequencies to be assigned sound physical values.

The final spectral resolution is measured over the spectra of the Th-Ar calibration lamp. Most of these lines are extremely narrow and the observed width in the extracted spectra of each one of those lines can be considered a correct measure of the Point Spread Function. A selected list of these lines is available in a highly precise Atlas used for wavelength calibration. It is this subset of well known lines that is used to measure the spectral resolution.

Every single line used in this measurement is fit with a function convolution of a Gaussian and a square window, supposed to represent the intrinsic super-resolved line width and the pixel. The variance of the Gaussian part is divided by 1.4155 to retrieve the equivalent resolution of the convolved PSF. Fig. 1 shows a typical measure of these resolutions line by line. Orders can be easily identified. The histogram of line resolutions affords a gaussian fit (Fig. 2). The announced resolution of the instrument is the maximum of this distribution of line resolutions. This histogram is made available in the PDF document collecting information for every stellar observation.

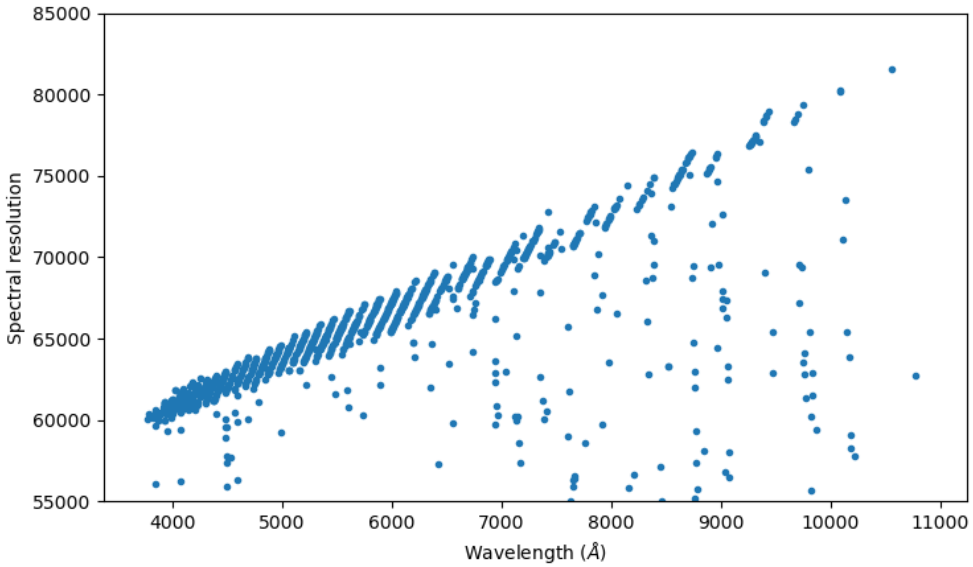

Figure 1: Measured spectral resolution on a typical calibration (October 5, 2023).

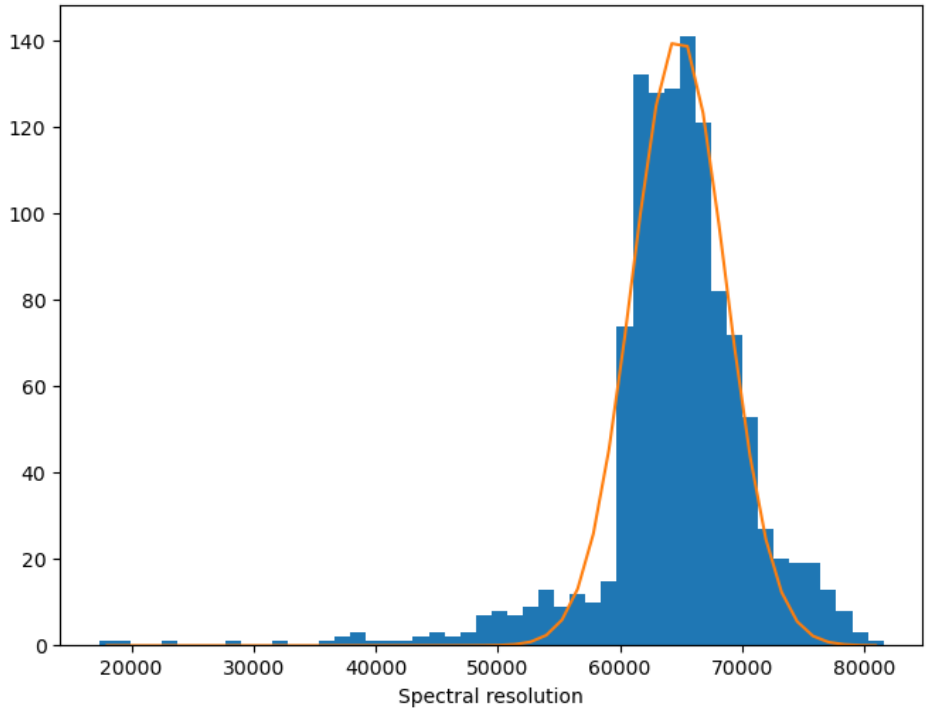

Figure 2: Histogram of spectral resolutions on a typical calibration (October 5, 2023). Overimposed, the Gaussian fit is shown whose maximum defines the announced spectral resolution of the instrument for that calibration

Wavelength calibration

Wavelength calibration is made order by order in a two-step process. The first step is a bootstrapping algorithm that, using an adjusted spectrograph law, tries and finds lines on a high precision atlas of Th-Ar lines made for UVES. The found lines are modelled with a second degree polynomial that is fed to the second step of calibration. In this second step, the lines of the atlas are identified modelled with a PSF function and a fifth degree polynomial is adjusted to the lines' position.

Given the dispersion polynomial we compute the error of each individual line in the atlas and build a histogram. A gaussian fit of this histogram is seen in Fig. 3. This is the error in velocity that is quoted in the logs, as in Fig. 4, where this error value is plotted for the daily calibrations of 2024.

This error is an error per line. If only one line were used for velocimetry the precision would be limited to these 40m/s seen in the figures. But many lines are used for the measurement. Since the errors per line are gaussian (ref the histogram in Fig. 3), they add up quadratically. **The accumulated error is of 2-3 m/s in average.**

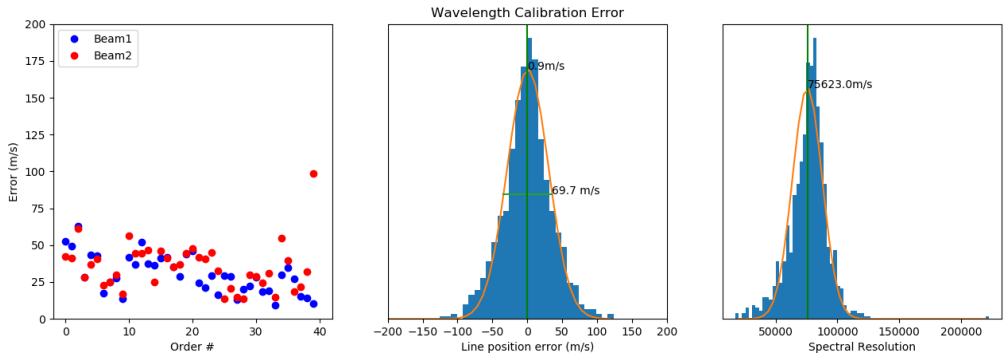

Figure 3: A calibration on December 13th 2024. At left: Average error per line at each order and beam. At center: histogram of position errors per line for all Th-Ar lines in the atlas. At right: histogram of the spectral resolution

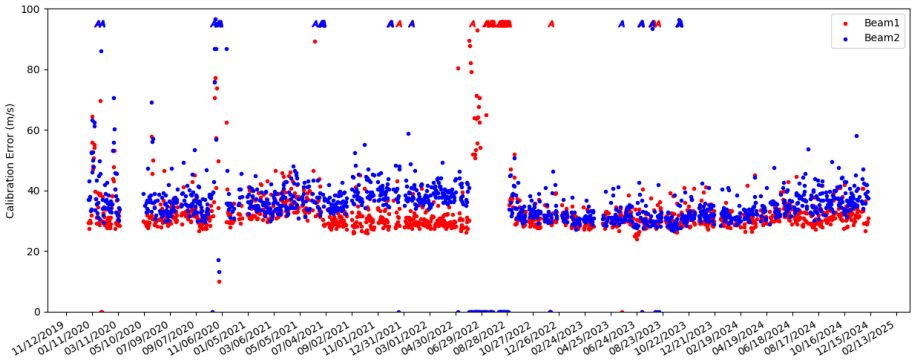

Figure 4: Average absolute wavelength calibration error, daily measured for the two beams, including through periods of spectrograph tests.

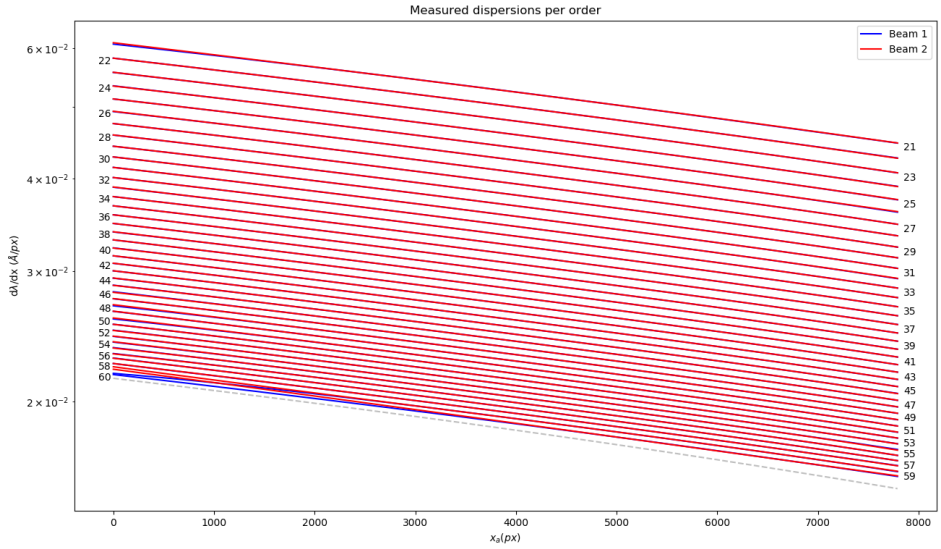

Figure 5: Dispersion at each order. Differences between the values in one and the other beam indicate places where the calibrations are faulty. Order 60 cannot be measured and is extrapolated from previous order (dotted line)

Part II

Stellar observations

Spectropolarimetry: β CrB

The star β Coronae Borealis is a magnetic calibration star. The main component of the system is the star A9 Sr Eu Cr (Renson & Manfroid 2009) with a radius and effective temperature of $2.63 \pm 0.09\,\mathrm{R}_\odot$ and $7980 \pm 180\,\mathrm{K}$, respectively (Bruntt et al. 2010).

The orbital period is $P = 3845.4 \pm 0.87$ d (10.4 a) and the rotation period is 18.482 d (Han et al. 2018). Bagnulo et al. (2000) concluded that the large-scale magnetic field geometry of the star can be described by a number of combinations of dipole and quadrupole fields. The longitudinal field has a peak-to-peak amplitude of about 1.5 kG.

Because of these characteristics, β CrB is regularly observed at TBL to validate the instrument. This is done through the I- and V-LSD profiles, computed from an A8p mask. Note that all the procedures described below are strictly the same for Narval and Neo-Narval data.

Concerning the I-profiles, all the line parameters (velocity, residual flux, full width and equivalent width) were computed from a gaussian fit. Results are shown on Fig 6:

- Radial Velocity: there is a full continuity between both instruments, as also represented on Fig. 7. The residuals may indicate that the used ephemeris of Han et al. (2018) is not exact enough yet.
- Residual Flux: there is a clear jump of about 4 % between the two instruments.
- Full Width at Half Maximum: the jump is even clearer, amounting to about 13 %
- Equivalent Width: exactely the same jump by also about 13 %

The magnetic field is computed from the first moment method, using the V-LSD profiles determined with the classical normaized weight vl.d.g

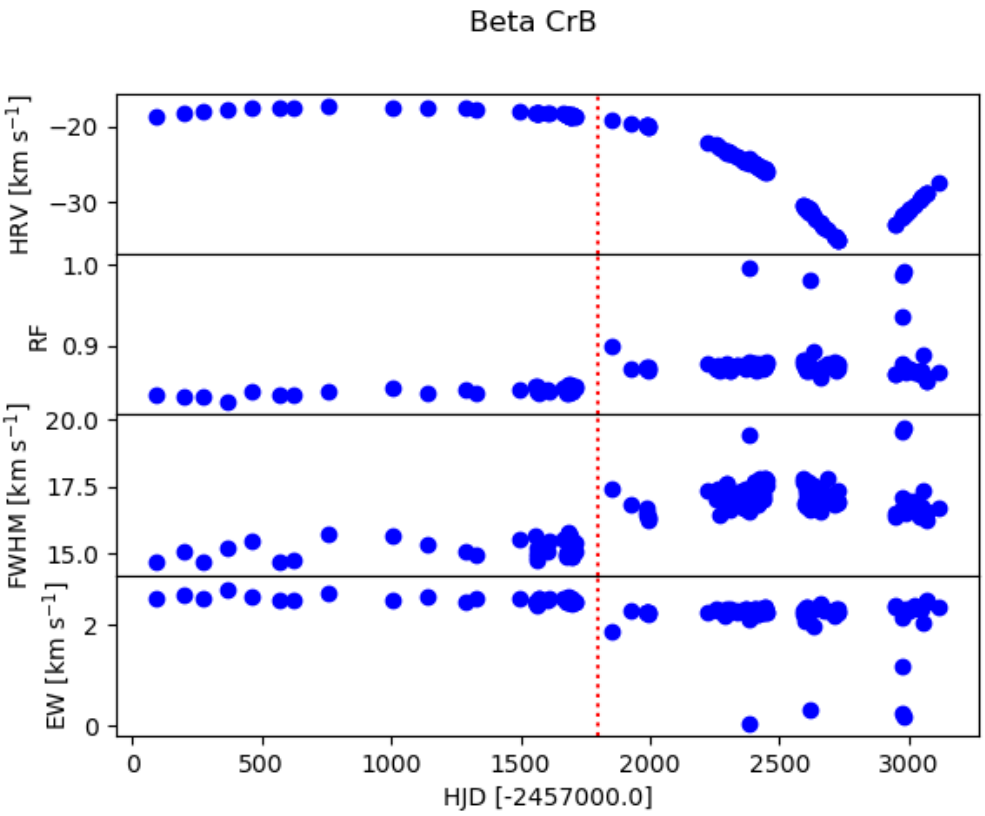

Figure 6: The different line parameters computed using a gaussian fit on the LSD profiles. The red dashed line is the frontier between Narval and Neo-Narval data.

Results are presented in Fig. 8.

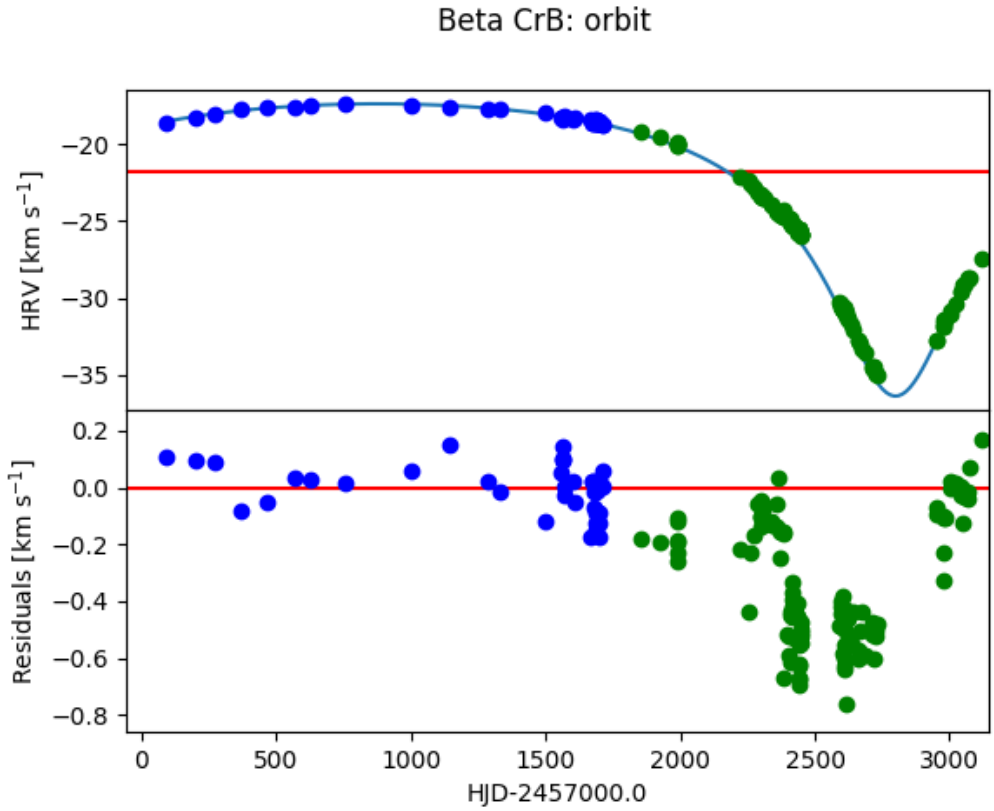

Figure 7: The solid curve represents the orbit computed from the orbital elements provided by Han et al. (2018), blue and green points show the measurements for Narval (blue) and Neo-Narval (green). Below are the residuals observations - model.

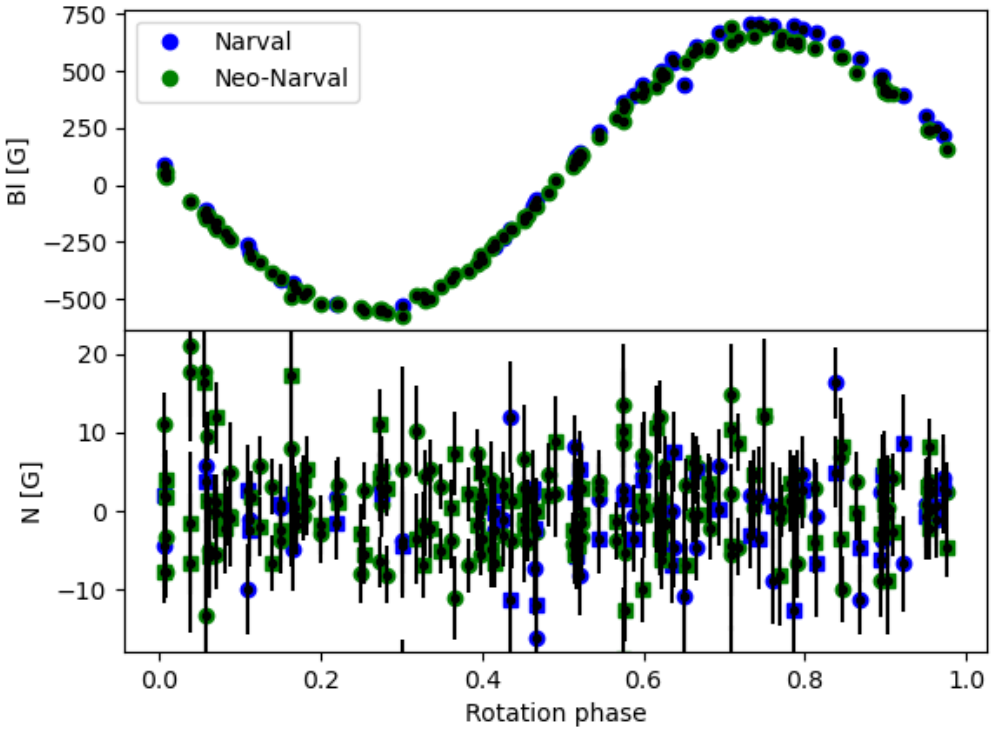

Figure 8: The upper plot shows B_ℓ as a function of the rotation phase. The bottom figure shows the corresponfing signal computed in the Null 1 signal. Below are the residuals observations - model.

Spectropolarimetry: Betelgeuse

The observation and analysis of linear polarisation in red supergiants and other evolved stars has taken a growing share of the observing time with NeoNarval, as it did with Narval in its last years.

Betelgeuse is the reference object for all those observations in many different senses. The comparison of the data obtained by NeoNarval to those taken by Narval has been made by López Ariste et al. (2022). Those authors conclude that there is no apparent difference in the linear polarisation data obtained with one or the other instrument.

In 2022 and 2023, Espadons at CFHT observed Betelgeuse. Within one week both before and after those observations, NeoNarval also observed Betelgeuse. In these two datasets we have therefore a good and direct comparison between on one side Narval, through its clone in Espadons, and the attached suite of data reduction codes and on the other side NeoNarval with its own and independent suite of codes.

The two figures 9 and 10 are organised identically. Three panels are shown for Q, U and V. In each panel three columns, ordered by date, show the observations of NeoNarval, identified with an N in front of the date, and Espadons, identified with an E. Stokes Q and U were observed twice sequentially by both instruments at each date. The two LSD profiles for the individual sequences are shown stacked vertically, while the addition of the two sequential profiles is shown in the bottom row of plots. In every plot, the Stokes signal is shown in a blue continuous line, while the Nulls are shown with dashed red and green lines. The case of Stokes V follows the same organisation with the only difference that 8 sequences were taken to try to reach the tiny Zeeman signal visible in this object. It is in this comparison of V that some differences beyond the noise may be seen, particularly in the data of 2022. At any rate, these differences remain below the 10^{-4} level. We must keep in mind that in linear polarisation changes in the polarization signal are seen in the time scale of one week. So it is not to be excluded that also in V such differences are just physical and not due to the instruments. Nevertheless, the

chapter of this work dedicated to the Nulls may bring another possible explanation to these differences.

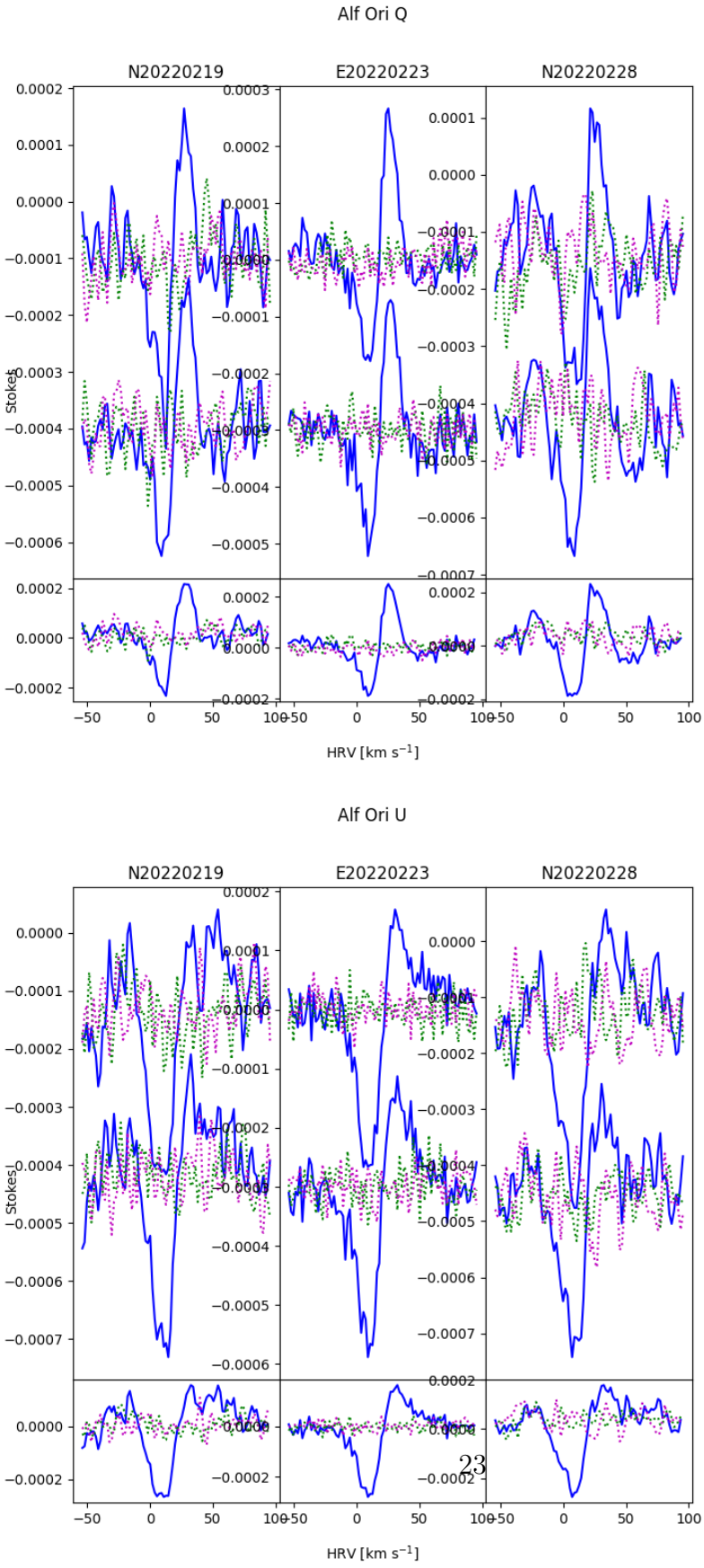

Figure 9: NeoNarval and Espadons observations of Betelgeuse in 2022. See the text for a detailed explanation of the different plots.

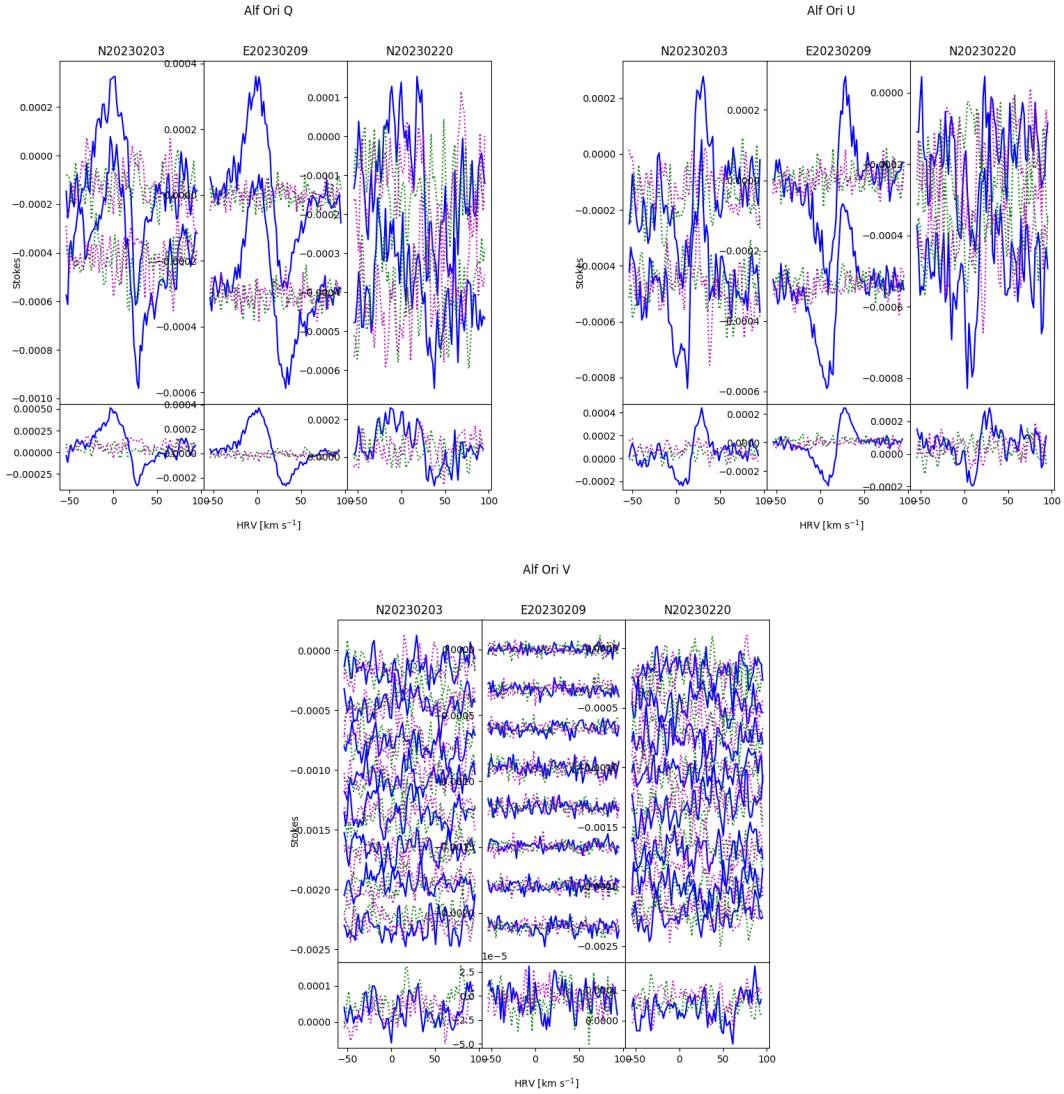

Figure 10: NeoNarval and Espadons observations of Betelgeuse in 2023. See the text for a detailed explanation of the different plots.

Spectropolarimetry: Vega

Perhaps the tiniest signal reliably detected by Narval was the Zeeman V signal seen in Vega (Lignières et al. 2006, Petit et al. 2020). It is therefore an interesting test for NeoNarval to recover such signal as well. No observation with the specific purpose of testing this limit has been made by us. However, Vega has been profusely observed with NeoNarval and enough data is available to make some quick-and-dirty exploration, in parallel to the work made by the PIs of those observations.

The data used here comes from observing time assigned to T. Böhm. The level 3 files automatically reduced with the DRS in real time were used. The real time DRS does an automatic LSD on the data with an automatically chosen mask. This mask appears to roughly correspond to the spectral type of Vega. But no further test or filtering of this mask has been attempted nor any re-computation of the LSD profile.

Data from August 4, 2023 through August 12 was added up just weighted by its signal-to-noise as determined by statistics over the Null profile. Fig. 11 shows the resulting LSD spectra. In spite of the crudeness of the analysis, a Zeeman V signal of amplitude and polarity comparable to the ones published with Narval data appears, while the Null signal is compatible with photon noise at 5×10^{-6} level. As the only difference with previously published data, the V profile is more complex with an extra lobe visible in the extreme wing of the line, a feature not found in any previous Narval observation. Whether real or not, this difference between Narval and NeoNarval appears at a level of 1×10^{-5}

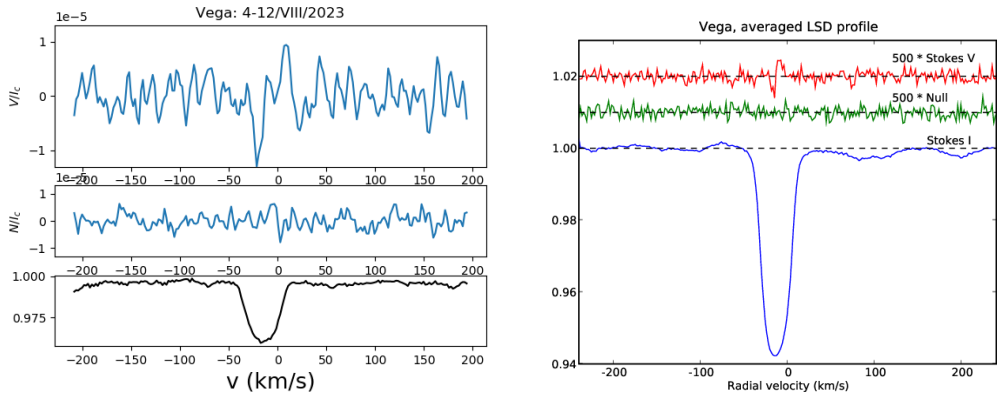

Figure 11: LSD Stokes V spectra of Vega. At left: addition of data taken in August 2023 with NeoNarval. At right: Profiles from Lignières et al (2006) with Narval.

Intensity profiles: EK Draconis and Altair

A recent study by Namekata et al (2024) deepens in the analysis of the Neo-Narval data by matching the observations with models and extracting images of the magnetic field of the star EK Dra. By matching physical models with the observed profiles, this work implicitly excludes instrumental effects on the final profiles, either in intensity or in Stokes V polarimetry.

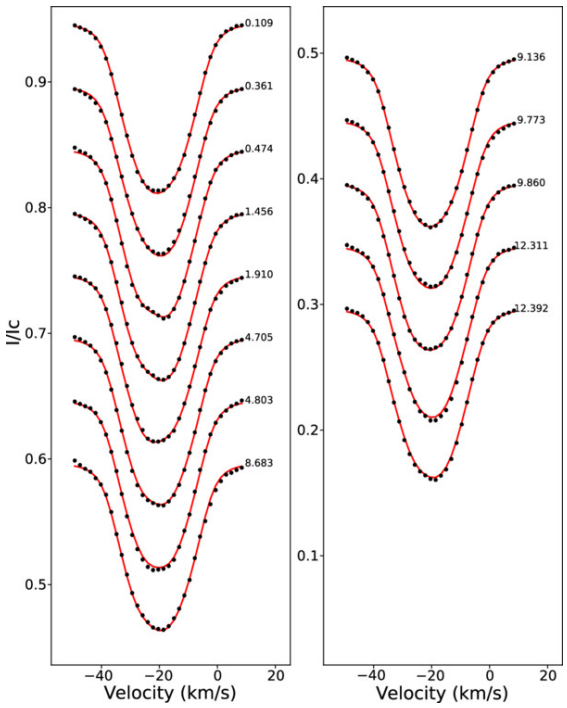

Figure 12: Stokes I profiles from a Neo-Narval time series of EK Dra. In red, the modelled profiles. Fig. 2 of Namekata et al (2024)

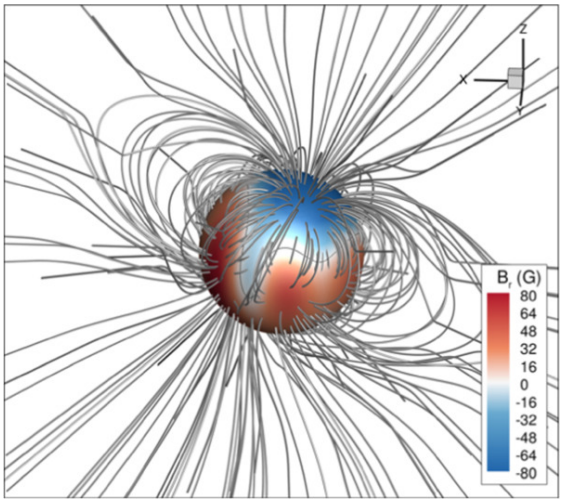

Figure 13: Photospheric magnetic field and the coronal extrapolation from Neo-Narval measurements. Fig. 4 of Namekata et al (2024)

Similar conclusions on the quality of the intensity profiles produced by Neo-Narval can be found in the work of Rieutord et al (2023). The fast rotating A-star Altair was observed by NeoNarval. Wiggles of an amplitude of 10^{-3} were found in the intensity profiles of the observed spectra, with a sensitivity of 2×10^{-4}. These wiggles were coherently followed over several nights revealing an oscillation pattern that was succesfully matched by the author's models on the oscillations of these rapidly-rotating stars

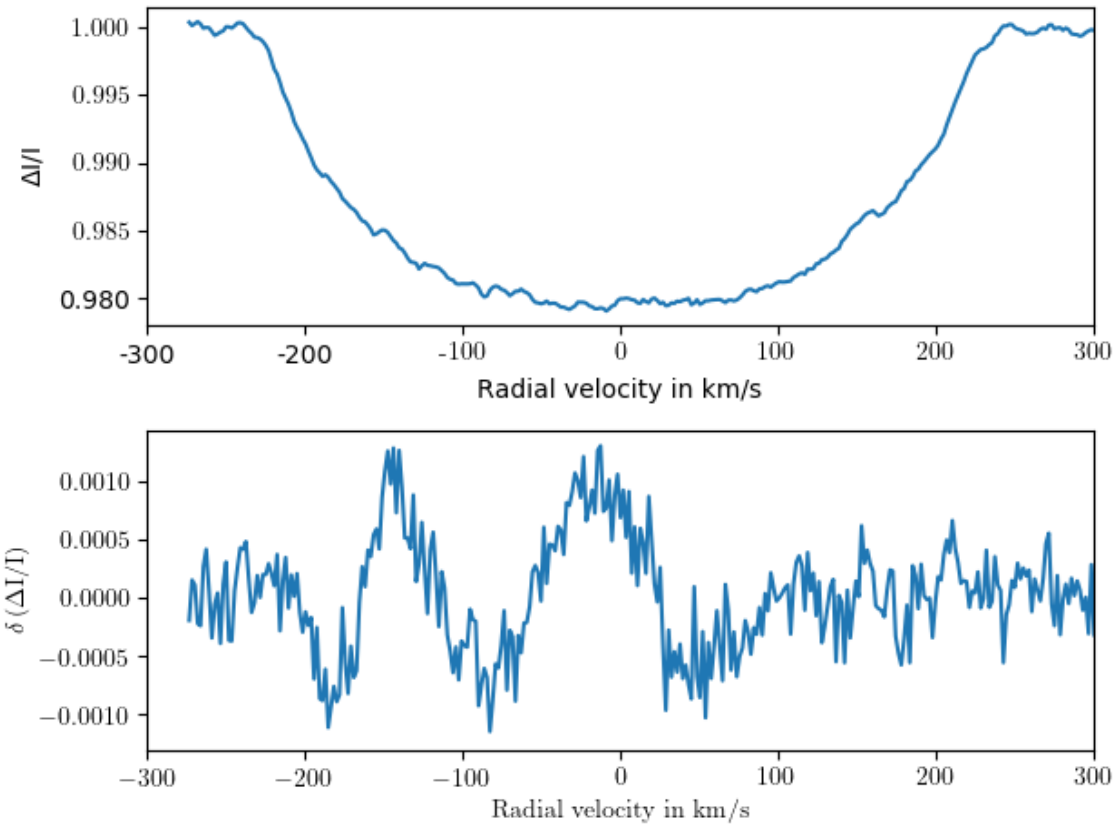

Figure 14: Example of Stokes I profiles observed by NeoNarval on Altair, and the tiny wiggles in them. Fig. 1 of Rieutord et al (2023)

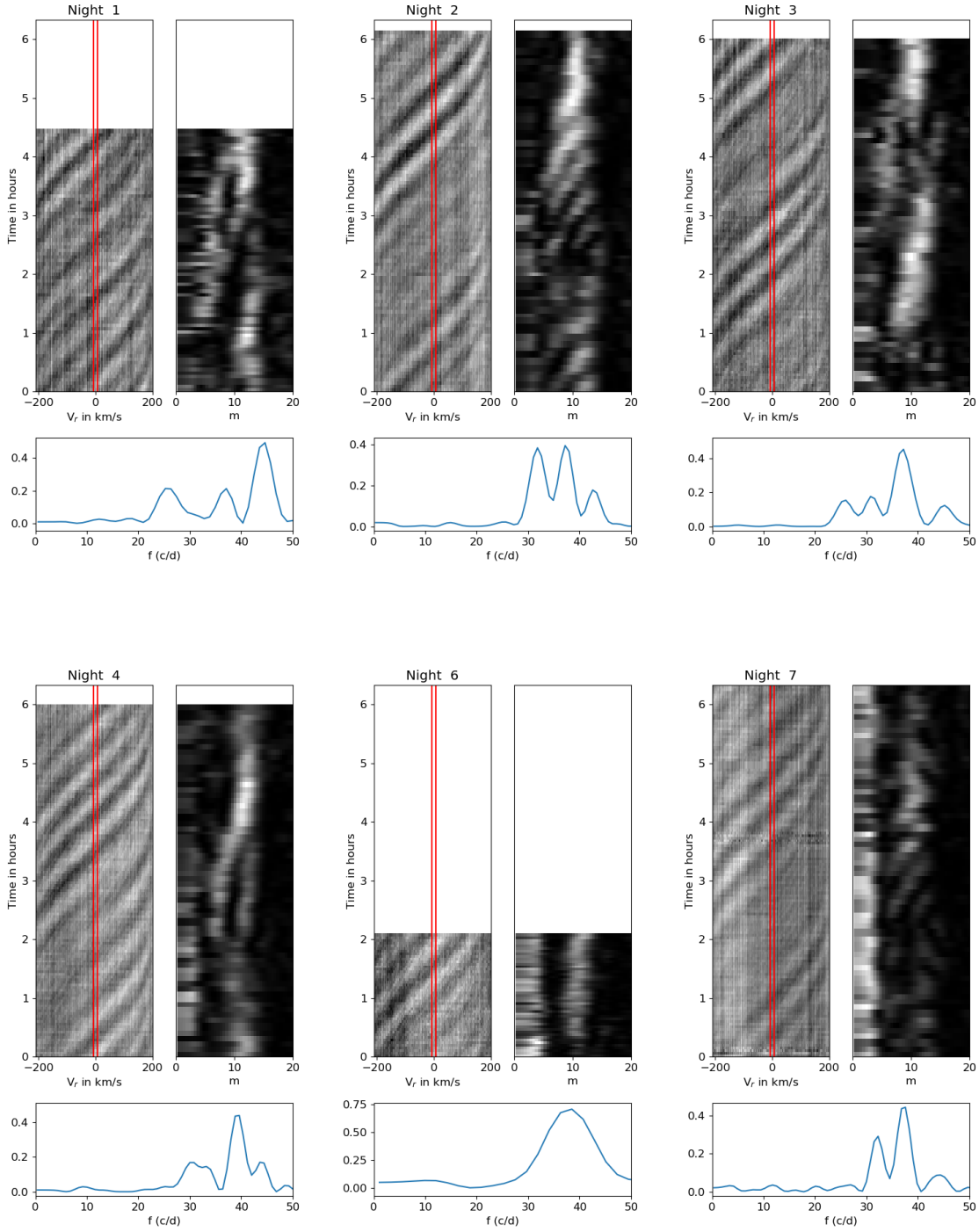

Figure 15: Follow-up of the wiggles on different nights as observed by NeoNarval. The oscillations thus unveiled fully match the theory of the oscillations on these rapidly rotating objects. Fig. 3 of Rieutord et al (2023)

.

Velocimetry

NeoNarval upgrade is justified, with respect to Narval, by the goal of attaing 3 m/s sensibility in the measurement of Doppler shifts in the lines of stellar spectra. It is a fact that the instrument was delivered with no demonstration of its performances on velocimetry nor any software to perform those measurements. NeoNarval velocimetry is therefore developed in less-than-optimal conditions. The present document presents the state of the art of velocimetry tests with NeoNarval and it is, hopefully, intended to evolve as the work on velocimetry unfolds painfully.

HD185144 is a well-known calibration star for velocimetry, stable at levels well beyond the goals of NeoNarval. It presents a magnetic signature which is also seen by NeoNarval and introduces a modulation on the measurements in individual exposures.

Figure 16 shows the ensemble of measurements made up to date on this reference star and analysed with the latest velocimetry code. Up to the summer of 2024 the dispersion of measurements was slightly better than $10m/s$. The culprit of this high dispersion was identified in the feedback circuit of the water chiller used to cool down the detector. A new chiller was acquired in September 2024. The right plot in Figure 16 shows the measures since, which, though still few in number show a dispersion of $3m/s$ approaching the specified target of NeoNarval

Simultaneously NeoNarval has measured the magnetic activity of the star. The resulting Stokes V profiles can be seen in 18. The combination of these two measurements is the goal of NeoNarval and is first illustrated here.

It is also interesting to show for HD185144 how the magnetic activity impacts the velocimetry. As NeoNarval rotates back and forth the waveplates of its polarimeter, the spectral line, burdened by the presence of alternatively positive and negative circular polarization, is shifted alternatively to the blue and to the red, something that the velocimetry code interprets as a velocity. NeoNarval has all the information to correct for this (Fig.16), but we can uncorrect for this and see the impact of magnetic activity in the measure of velocities in Fig. 17

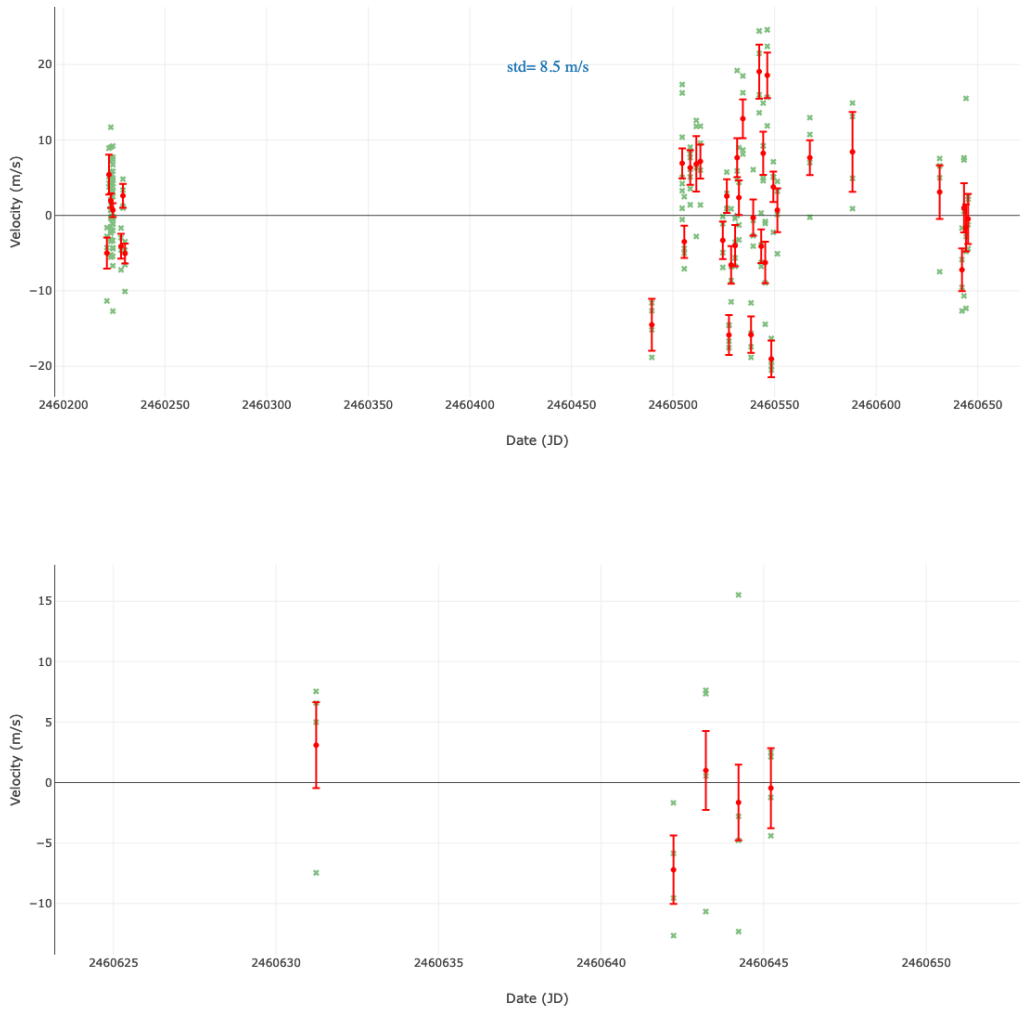

Figure 16: Velocimetry on a series of observations of HD185144. Top, full series of measurements since the spring of 2023, with a noise of 8.5m/s. Bottom, measurements since the change of the water chiller, improving noise down to 3m/s.

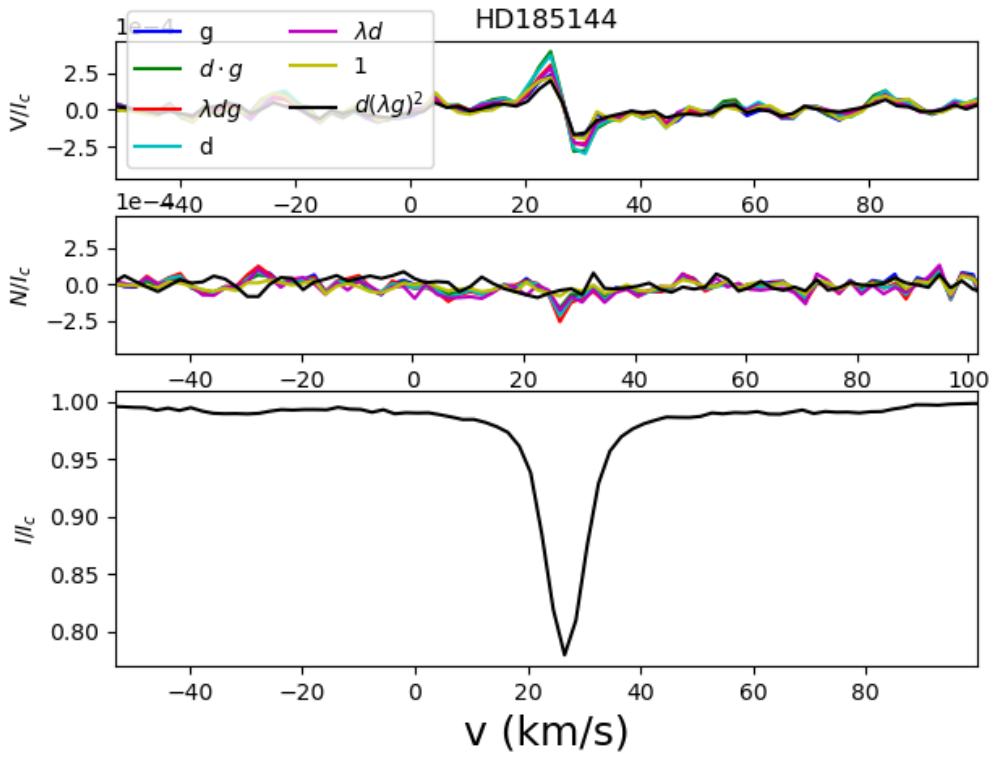

Figure 17: LSD signal of HD185144. From top to bottom, Stokes V, Null and Intensity. Several weights are shown together for comparison.

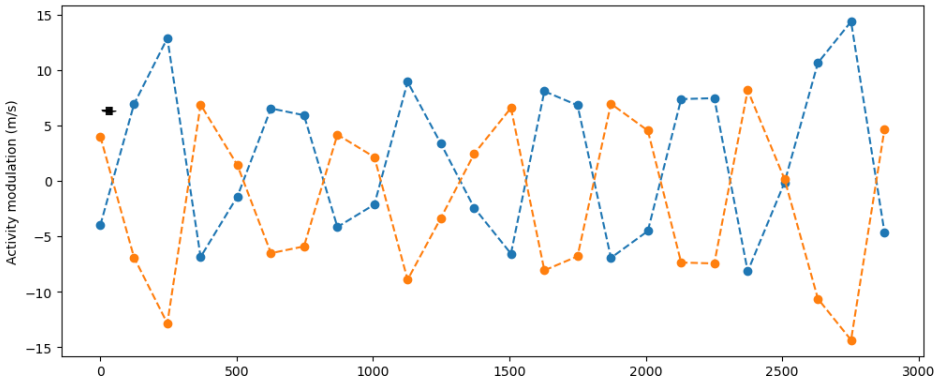

Figure 18: Velocimetry of beams 1 (blue) and 2 (orange) after subtraction of the average of the two signals, what leaves only the polarimetric modulation.

Although not yet at the required precision level, Neo-Narval can see exoplanets and attempt spectropolarimetry on them. The following figures show the measured orbits of three easy exoplanets with diminishing amplitude. Most of the differences with the theoretical orbits are attributed in the litterature to stellar activity and not to measurement errors.

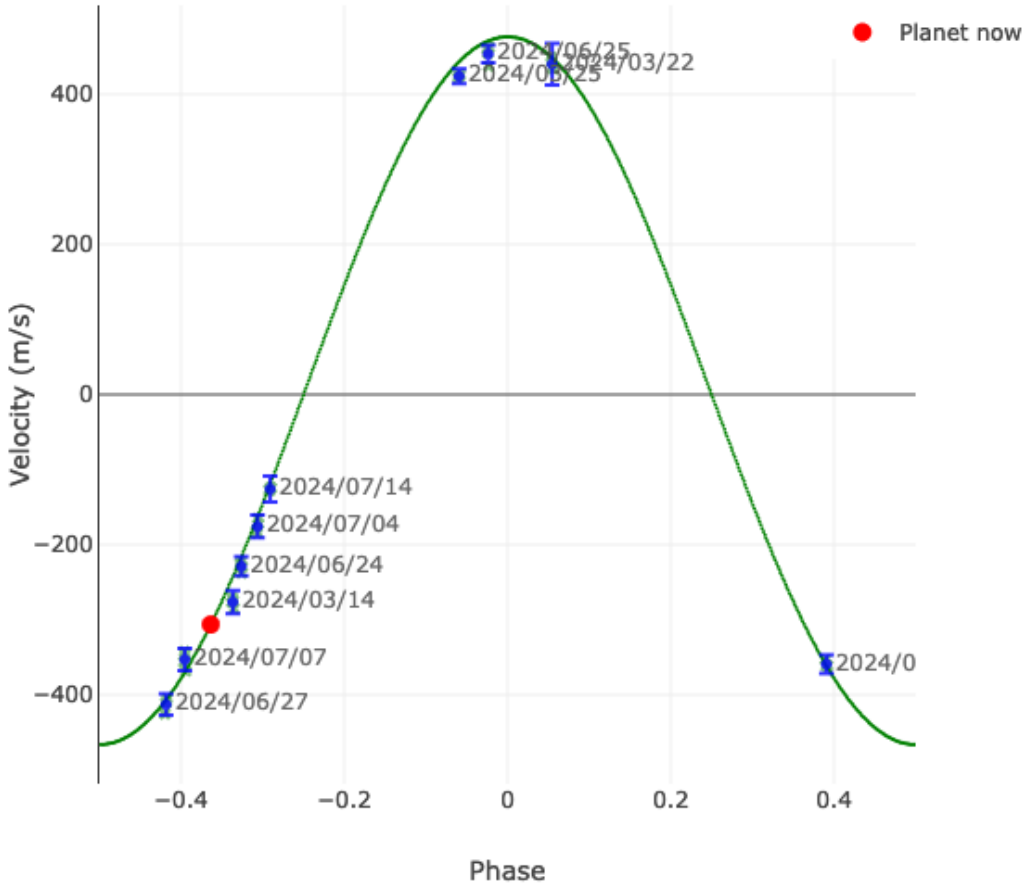

Figure 19: Velocimetry of the star τ Boo with the orbit of its planet

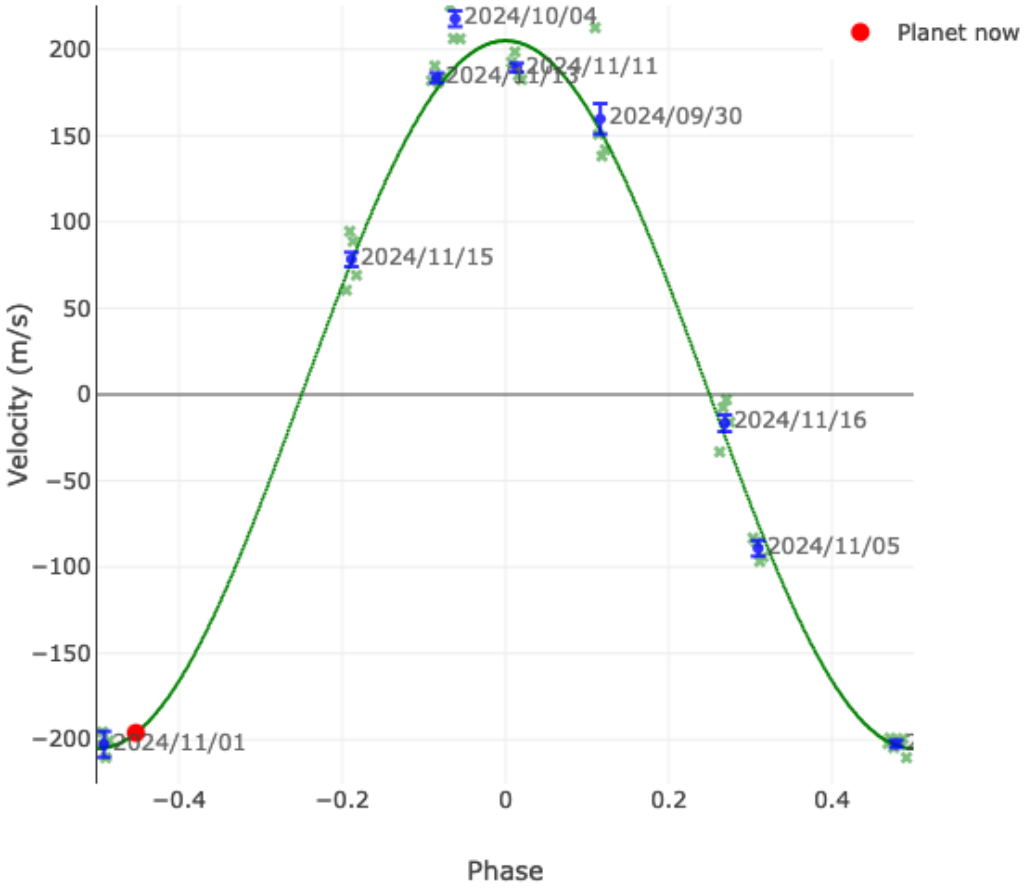

Figure 20: Velocimetry of the star HD189733 with the orbit of its planet

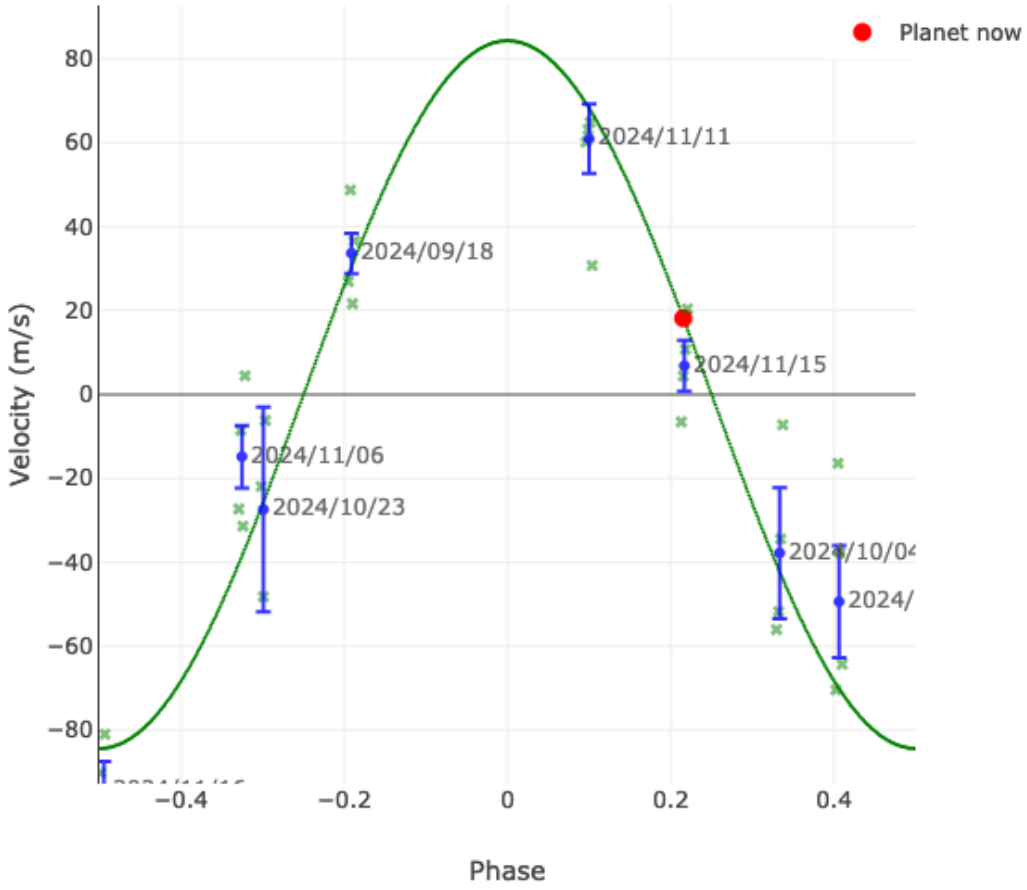

Figure 21: Velocimetry of the star HD209458 with the orbit of its planet